



ARTICLES/ARTIGOS/ARTÍCULOS/ARTICLES

Change vector analysis to detect deforestation and land use/land cover change in Brazilian Amazon

Master Pedro José Farias Fernandes  
Universidade Federal Fluminense – Instituto de Geociências Laboratório de Geografia Física – Av. Gal. Milton Tavares de Souza s/nº - CEP: 24210-346 - Niterói - RJ, Brasil. E-mail: pj\_fernandes@id.uff.br

Master Luiz Felipe de Almeida Furtado  
Instituto Nacional de Pesquisas Espaciais – INPE - Caixa Postal 515 - 12227-010 – São José dos Campos - SP, Brasil. E-mail: chefechefe@gmail.com

Master Raphael e Silva Girão  
Universidade Federal do Rio de Janeiro – Departamento de Geologia - Av. Athos da Silveira Ramos 274 - 21941-916 - Rio de Janeiro – RJ, Brasil. E-mail: raphaelgirao@hotmail.com

RESUMO

ARTICLE HISTORY

Received: 26/02/2014  
Accepted: 10/11/2014

PALAVRAS-CHAVE:  
Análise por Vetor de Mudança  
Desmatamento  
Sensoriamento Remoto

O presente trabalho tem como objetivo utilizar a Análise por Vetor de Mudança para detectar desmatamentos e outras mudanças no uso e cobertura da terra entre os anos de 1989 e 2010 no município de Tapurah/MT a partir de dados TM/LANDSAT-5. Como resultado, obteve-se um mapa de mudanças no uso e cobertura da terra no período mencionado, que permitiu a identificação satisfatória das áreas de desmatamento em Tapurah, apresentando índice Kappa de 0,6464 e 33,9% de área desmatada.

KEY-WORDS:  
Change Vector Analysis  
Deforestation  
Remote Sensing

ABSTRACT: CHANGE VECTOR ANALYSIS TO DETECT DEFORESTATION AND LAND USE/LAND COVER CHANGE IN BRAZILIAN AMAZON. This study aims to use the Change Vector Analysis to detect deforestation and other changes in land use and land cover between 1989 and 2010 in the municipality of Tapurah/MT from TM/Landsat-5 data. As a result, we obtained a map of change in land use and land cover in the aforementioned period, which allowed the identification of areas of deforestation satisfactorily in Tapurah, with kappa index 0.6464 and 33,9% of deforestation.

RESÚMEN:  
Análisis de Vector de Cambio  
Deforestación  
Teledetección

RESÚMEN. ANÁLISIS DE VECTOR DE CAMBIO PARA DETECTAR DEFORESTACIÓN Y CAMBIOS EN EL USO Y COBERTURA DE LA TIERRA LA EN LA AMAZONIA BRASILEÑA. Este trabajo tiene como objetivo utilizar la análisis de vector de cambio para detectar la deforestación y otros cambios en el uso y cobertura de la tierra entre los años 1989 y 2010, en el municipio de Tapurah/MT, a partir de datos TM/Landsat-5. Como resultado, se obtuvo un mapa de los cambios en el uso del suelo y la cubierta vegetal en el período mencionado, lo que permite identificar áreas de deforestación en Tapurah, con estadística kappa de 0,6464, y 33,9% de superficie deforestada.

---

## Introduction

Agricultural activities are highlighted in the Brazilian economy since the country is one of the largest grain producers in the world. The expansion of agriculture is a reality in Brazil, mainly in the Midwest, where agriculture incorporated areas of the Brazilian savannah (JEPSON, 2005), and is entering the Amazon biome. Despite the economic benefits of the growth of agribusiness, agricultural activities can cause severe environmental impacts such as deforestation and soil erosion (GUERRA, 2007).

Consequently, the entry of agriculture in the Amazon changes the landscape, which causes changes in land use and land cover. Within this perspective, Remote Sensing has emerged as a data source of the surface that allows the detection and study of landscape change, particularly by facilitating the monitoring of phenomena using data from different dates. As the satellites provide a permanent collection and storage of data, it is possible to detect land use and land cover changes (LULC) in a given area at a given time (PRAKASH; GUPTA, 1998).

In Remote Sensing, techniques for change detection can be used to verify changes in LULC and deforestation. Change detection can be defined as the process of identifying differences in the state of an object or phenomenon through its observation at different times (SINGH, 1989).

For Singh (1989), there are two basic approaches to detect changes: (1) comparative analysis of independent classifications for each date and (2) simultaneous analysis of multitemporal data. This division is similar to that proposed by Johnson and Kasischke (1998), in which the techniques can be grouped into two classes: (1) based on spectral categorization (classification) of the input data and (2) techniques based on radiometric changes between images of different dates, as the ratio of bands, difference of bands, difference of images derived from transformation of bands (e.g., vegetation indices), regression, Principal Component Analysis and Change Vector Analysis (CVA).

CVA is a technique established and used by several authors (XIAN et al. 2009; BAYARJARGAL et al. 2006; ALLEN; KUPFER, 2000; SOHL, 1999; MALILA, 1980). A change vector can be obtained at a spectral feature space by differencing the values of the same pixel at different times (JOHNSON; KASISCHKE, 1998). CVA allows the identification of the nature of change as well as its magnitude, and is considered a robust tool for radiometric detection of changes, once it accepts as input n bands or transformed images of diverse origins (JOHNSON; KASISCHKE, 1998).

The present work admits the hypothesis that CVA allows the efficient detection of deforestation in Amazonia caused by agricultural expansion. Therefore, the aim is to use the CVA to detect deforestation and other changes in LULC between 1989 and 2010 in the municipality of Tapurah (MT) from TM/Landsat-5 data.

## Study area

The municipality of Tapurah is located in the State of Mato Grosso, Brazil (figure 1). According to data of 2010 from Brazilian Institute of Geography and Statistics (IBGE), Tapurah has 10.392 inhabitants and an area of approximately 4.510 km<sup>2</sup>. According to

data from the Agricultural Census of 2006, the city stands out mainly for the production of grains (specially the cultivation of soybeans).

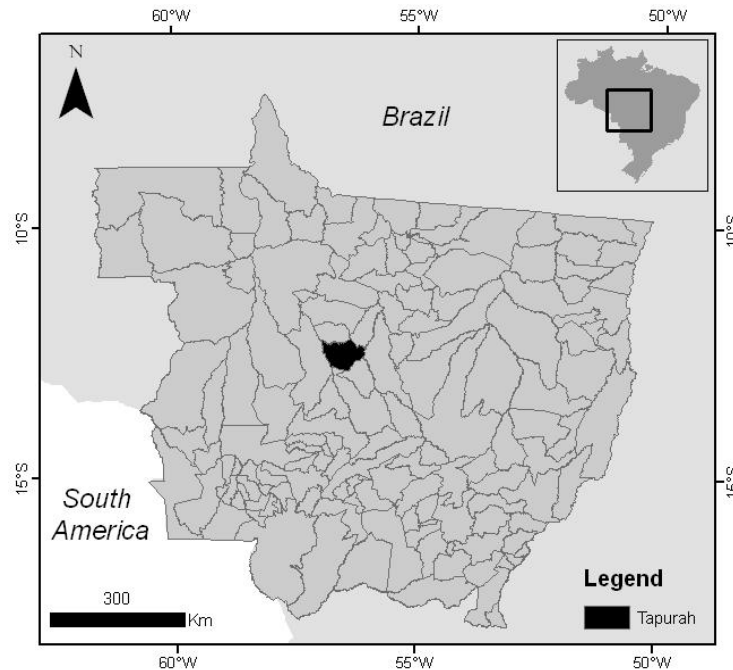


Fig. 1 – Localization of Tapurah

The study area is included in the Amazon biome, and has a hot and humid climate: the type Aw according to Köppen classification, with a dry season between May and August. According to the project RADAMBRASIL, the vegetation can be characterized by semideciduous forest in the contact ombrofile forest/stationary forest. However, its vegetation is suffering from deforestation caused by expansion of agriculture, so Brazilian Institute of Environment and Renewable Natural Resources (IBAMA) considers the location as a priority for surveillance operations (MESQUITA JR et al., 2007).

#### Material and methods

To reach the objective of the study, the methodology followed the steps in the flowchart below (figure 2):

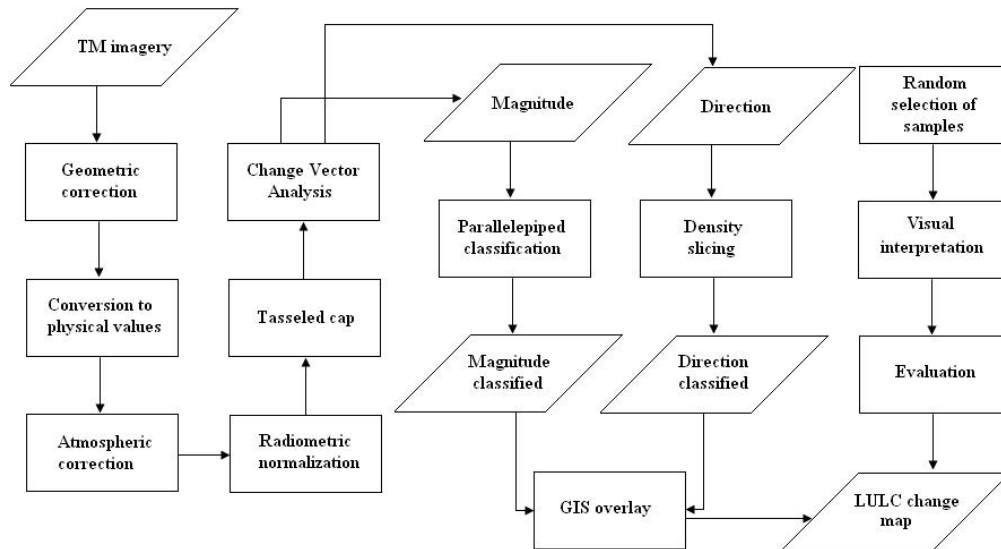


Fig. 2 – The flowchart of activities

## Material

Two images of the TM sensor onboard the Landsat 5, bands 1, 2, 3, 4, 5 and 7, of the path/row 227/69, were used. The images are from the dates of 21/07/1989 and 31/07/2010 and have a spatial resolution of 30 meters, covering an area of 185x185 km. The images can be found on the website of the image catalog from INPE (<http://www.dgi.inpe.br/CDSR/>).

Images of close dates were selected to reduce the effects of variability that are not of interest, making the process of change detection more accurate (JOHNSON; KASISCHKE, 1998; SINGH, 1989).

## Methods

### Pre-processing

This step involves geometric correction, conversion to physical values, atmospheric correction and radiometric normalization, in order to minimize errors in the final result.

A precise geometric correction is necessary for change detection (LU et al., 2004). The 1989 image was referenced based on 2010 image, accepting the Root Mean Square Error (RMSE) less than one pixel (JIANYA et al., 2008). For this operation, an affine function and resampling by nearest neighbor interpolation were employed, thereby new digital numbers (DN) values are not created, what saved the radiometry of the scene targets.

The conversion to physical values was applied in order to have a better spectral characterization of the targets, as well as providing images and calculations of different bands, because the DNs of an image are not on the same scale as the others (PONZONI; SHIMABUKURO, 2009). To do this, the apparent radiance (Equation 1) and apparent reflectance (Equation 2) equations were used:

$$L_0(\lambda) = [L_{min}(\lambda) + \frac{(L_{max}(\lambda) - L_{min}(\lambda))}{2^x}] * DN \quad (1)$$

Where:  $L_0(\lambda)$  = apparent radiance;  $L_{min}(\lambda)$  = minimum spectral radiance;  $L_{max}(\lambda)$  = maximum spectral radiance; x = number of bits; DN = digital number.

$$\rho_a = \frac{\pi * L_0(\lambda) * d^2}{E_{sun}(\lambda) * \cos\theta} \quad (2)$$

Where:  $\rho_a$  = apparent reflectance;  $L_o(\lambda)$  = apparent radiance; d = earth-sun distance in astronomical units;  $E_{sun}(\lambda)$  = mean solar exoatmospheric irradiances;  $\theta$  = solar zenith angle

The coefficients Lmin ( $\lambda$ ) and Lmax ( $\lambda$ ), proposed by Chander and Markham (2003), can be found in Table 1 and Table 2 below.

Band	Lmin	Lmax
TM 1	-1,52	152,10
TM 2	-2,84	296,81
TM 3	-1,17	204,30
TM 4	-1,51	206,20
TM 5	-0,37	27,19
TM 7	-0,15	14,38

TABLE 1 – COEFFICIENTS IN W/(m<sup>2</sup>. sr .  $\mu$ m) APPLIED FROM 01/03/1984 TO 04/05/2003.  
Source: Chander and Markham (2003)

Band	Lmin	Lmax
TM 1	-1,52	193,0
TM 2	-2,84	365,0
TM 3	-1,17	264,0
TM 4	-1,51	221,0
TM 5	-0,37	30,2
TM 7	-0,15	16,5

TABLE 2 – COEFFICIENTS IN W/(m<sup>2</sup>. sr .  $\mu$  m) APPLIED FROM 05/05/2003.  
Source: Chander and Markham (2003)

The atmospheric correction was applied in order to mitigate the atmospheric effects, making it possible to obtain the surface reflectance. The method used was proposed by Chavez (1988), known as the Dark Object Subtraction (DOS). The method of Chavez (1988) was applied by defining set of pixels that must take the value 0. According to Shimabukuro and Ponzoni (2009), one of the main criticisms of this method is the fact that it only considers the scattering, and the atmospheric effects are constant over the entire image. However, it was not possible to use more complex models that consider atmospheric absorption, because it would be necessary to know the atmospheric parameters at the time of image acquisition. And the use of incorrect parameters can produce errors in multitemporal analysis (CASTILLO, 2011; JESUS, 2009).

In order to obtain an accurate radiometric calibration, multitemporal data were radiometrically normalized to present spectral compatibility, using the 2010 image as reference. According to Shimabukuro and Ponzoni (2009), conversion to surface reflectance is not sufficient for multitemporal spectral characterization of surface targets, because the values of surface reflectance is influenced by variations in the geometry of data acquisition and the influence of nonlinear variations concerning sensor calibration. To mitigate this effect, the radiometric normalization method proposed by Hall et al. (1991) was applied. The method consists of a linear regression of a constructed data set consisting of bright and dark targets in each band, invariant over time, such as shadows, water bodies, roads and bare soil (CASTILLO, 2011; PONZONI; SHIMABUKURO, 2009). For this linear transformation, the following equations were used:

$$T_i = m_i * x_i + b_i \quad (3)$$

Where:

$$m_i = \frac{(B_{ri} - D_{ri})}{(B_{si} - D_{si})} \quad (4)$$

$$b_i = \frac{(D_{ri} * B_{si} - D_{si} * B_{ri})}{(B_{si} - D_{si})} \quad (5)$$

Where:  $T_i$  = reflectance of the normalized image,  $x_i$  = reflectance of the original image;  $B_{ri}$  = average of the reference set of light targets;  $D_{ri}$  average of the reference set of dark targets;  $B_{si}$  = average of the light targets set to be normalized;  $D_{si}$  = average of the dark target sets to be normalized;  $i$  = bands of the sensor.

For the selection of sets in order to apply linear transformations, bright and dark pixels are selected at the edges of the scatter plot between the components Greenness and Brightness generated by Tasseled Cap transformation, using the coefficients proposed by Crist and Cicone (1984) (Table 3). Thus, the radiometric normalization procedure was applied to the multitemporal data, with the image from 2010 as reference.

### The Tasseled Cap transformation

Originally, the Tasseled Cap Transformation is a unique orthogonal transformation of MSS data into a space of four dimensions, which isolates the development of vegetation (green development), the yellow material (yellow development), the brightness of the soil (soil brightness), and reduce the dimensionality of the data (KAUTH; THOMAS, 1976), allowing better separability between targets such as bare soil and vegetation (CASTILLO, 2011).

Kauth and Thomas (1976) propose the Tasseled Cap transformation to describe the spectral and temporal trajectory of the targets of an agricultural scene, resulting in a design with a shape that resembles a gnome hat (GLERIANI et al. 2003; KAUTH; THOMAS, 1976). According to Kauth and Thomas (1976), Tasseled Cap transformation is a linear transformation with a fixed specific

matrix of transformation. Thus, unlike the PCA, the transform coefficients are fixed, and are first obtained by calculating the spectral variability of soil present in a scene, and following axes are the result of successive orthogonalizations of the plane of soils (GLERIANI et al., 2003).

With the advent of the TM sensor, which has six reflective bands, Crist and Kauth (1986) obtained the coefficients of transformations for the TM data, through a space hexadimensional, in Greenness component (related to vegetation greenness), Brightness component (related to the brightness soil) and Wetness (related to moisture content). The other components have no practical significance (GLERIANI et al., 2003).

The Tasseled Cap transformation was used to generate the Brightness and Greenness components, using the coefficients shown in Table 3.4, proposed by Crist and Cicone (1984) for TM data, which served as input data to the CVA.

### Change Vector Analysis

As seen earlier, CVA is a robust technique to detect radiometric changes, which allows the generation of an image of the magnitude of change (related to the magnitude of the vector) and an image of the direction of change (related to the direction of the vector).

Component	TM1	TM2	TM3	TM4	TM5	TM7
Brightness	0,3037	0,2793	0,4343	0,5585	0,5082	0,1863
Greenness	-0,2848	-0,2435	-0,5436	0,7243	0,0840	-0,1800

TABLE 3 - COEFFICIENTS FOR THE TASSELED CAP TRANSFORMATION FOR TM DATA

CVA accepts as input n bands, bands that can be original or transformed images (JOHNSON; KASISCHKE, 1998). Thus, in a radiometric attributes space, the change vector is formed between points corresponding to the same pixel at different dates (figure 3). A threshold value can be chosen for the magnitude of the vector to establish whether or not there was a change.

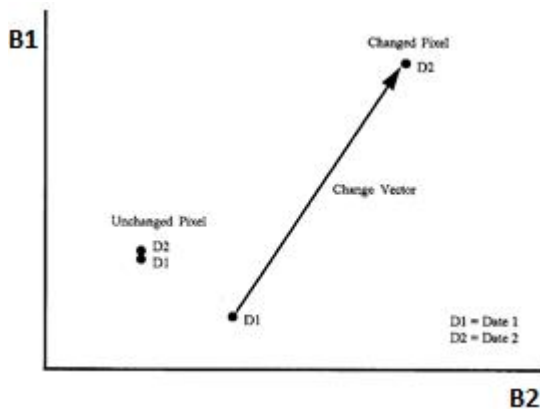


Fig. 3 – Change vector formed between two points corresponding to the same pixel at different dates. Source: Johnson and Kasischke (1998)

As the input data were the Greenness and Brightness components, produced by the Tasseled Cap transformation, for the generation of images of magnitude, Equation 6 was used, which corresponds to the magnitude of the change vector in a bi-dimensional space of radiometric attributes.

$$M = \sqrt{[(B_1 - B_0)^2 + (G_1 - G_0)^2]} \quad (6)$$

Where:  $M$  = change vector magnitude;  $(B_1 - B_0)$  and  $(G_1 - G_0)$  represent the difference between the Brightness and Greenness components, respectively, among the most recent year and a year earlier.

The direction of the vectors of change (Figure 3) is determined by angles that vary with the number of bands used as input to the CVA. Thus, there are positive and negative angles that enable the identification of  $2n$  classes of LULC changes, where  $n$  is the number of bands used as input in the model (MICHALEK; STOFFLE, 1993). In this paper, two images were used as input (Brightness and Greenness), thus an image with four classes of direction was generated. Therefore, to calculate the direction of the vectors of change in a two-dimensional space, the following equation (Equation 7) was used.

$$\alpha = \arctg\left[\frac{(B_1 - B_0)}{(G_1 - G_0)}\right] \quad (7)$$

Where  $\alpha$  = horizontal angle between a range from  $-180^\circ$  to  $180^\circ$  or from 0 to  $360^\circ$ ;  $(B_1 - B_0)$  and  $(G_1 - G_0)$  represent the difference between the Brightness and Greenness components, respectively, among the most recent year and a year earlier.

As the interest was to create a threshold between change and no change in the magnitude image, the parallelepiped classification was employed to generate this threshold. The image direction was density-sliced in accordance with variations of the gain and loss in Brightness and Greenness, so there are four quadrants established, which identifies four directions (figure 4). After this step, an overlay in GIS environment was carried out between the magnitude and direction to generate the final map of LULC changes.

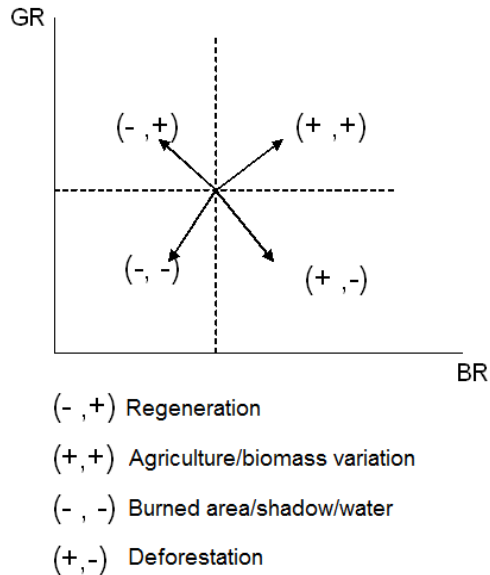


Fig. 3 – Change direction classes, where GR = Greenness and BR = Brightness.  
 Source: Adapted from Jesus (2009)

### Evaluation

115 points in the images were randomly selected in TM/Landsat 5 imagery, and those corresponding to clouds or doubtful areas were excluded, leaving 107 points. Later, from RGB color composites, each point was labeled in accordance to the classes identified for change by interpretation of the images. Thus, the LULC changes map was evaluated with the Kappa index, which defines a measure of accuracy according to the proportion of an area that is correctly classified based on a reference, in case the randomly selected points (CONGALTON, GREEN, 2003; CONGALTON, 1991). Thus, the Kappa index ranges from 0 (very weak classification) to 1 (an excellent rating), according to Landis and Koch (1977), allowing the evaluation of the maps use change and land cover generated (Table 4).

Kappa index	Classification quality
> 0	Poor
0 – 0,2	Slight
0,2 – 0,4	Fair
0,4 – 0,6	Moderate
0,6 – 0,8	Substantial
0,8 - 1	Almost perfect

Table 4 – Classification evaluation  
 Source: Landis and Koch (1977)

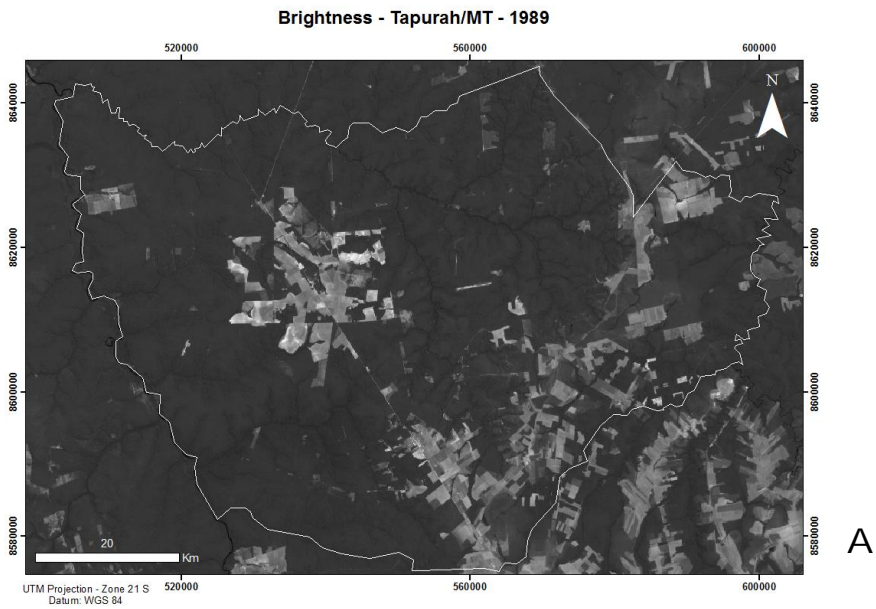
### Results

### Appreciation of data

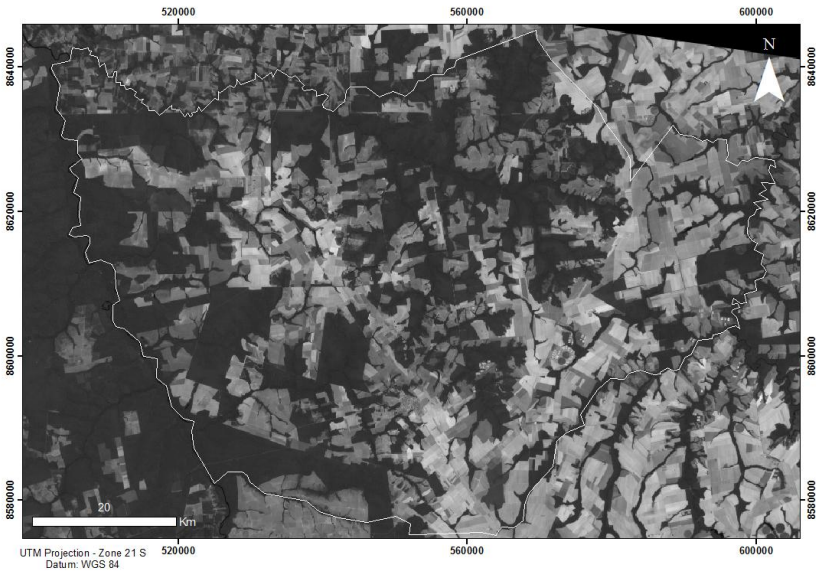
By examining the Brightness and Greenness component for the years 1989 and 2010, it was noticed there was an increase of deforestation caused by expansion of agriculture (figure 4).

### Change Vector Analysis

The CVA has generated two images, one of magnitude and direction of change vectors. The magnitude image is linked to the intensity change. Thus, a threshold between change and no change was established by parallelepiped classification, which generated a binary image with two classes (figure 5).

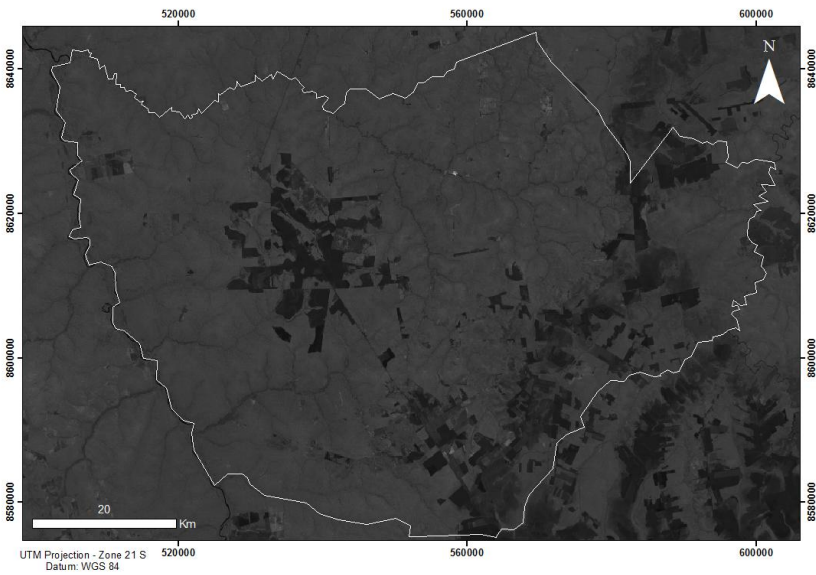


**Brightness - Tapurah/MT - 2010**



B

**Greeness - Tapurah/MT - 1989**



C

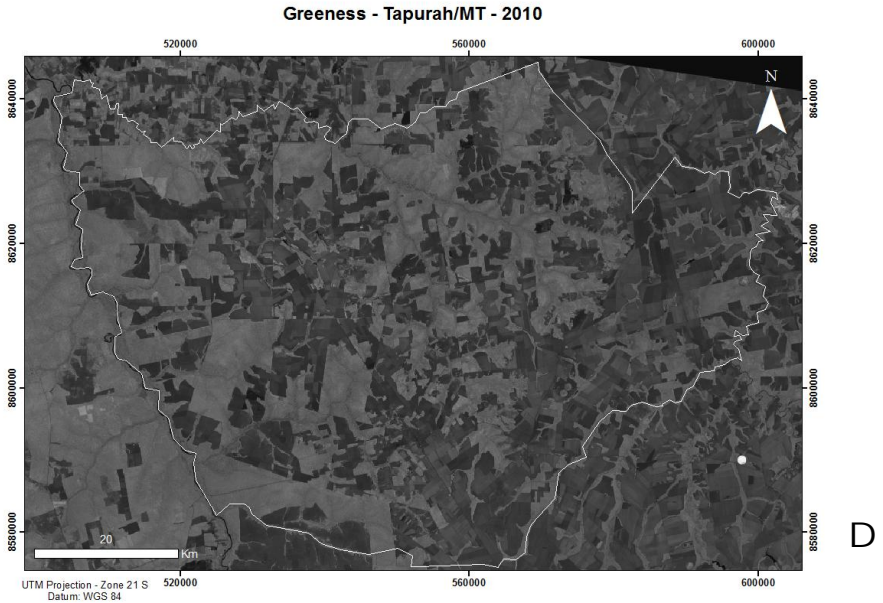


Fig. 4 – (A) Brightness component for 1989, (B) Brightness component for 2010, (C) Greenness component for 1989, (D) Greenness component for 2010. Note that deforestation increased between these years due to the entry of agriculture on forest areas.

The image of direction is associated with the nature of change, i.e., the kind of change, resulting in rasters ranging from -3,14 to 3,14. By application of density slicing, an image with four classes was obtained (Figure 6): Regeneration, biomass variation, burned areas/shadow/water and deforestation. Each quadrant (Figure 3) represents a class according to the angles of the change vector (Table 5).

LULC change	Range of angles
Biomass variation	From 0 to 1,57
Regeneration	From 1,57 to 3,14
Burned areas/shadow/water	From -3,14 to -1,57
Deforestation	From -1,57 to 0

TABLE 5 – Classes of change vector direction

Thus, Regeneration represents a drop in Brightness and an increase in Greenness. Biomass variation represents an increase in Brightness and in Greenness, indicating variations in the amount of biomass that can be associated with changes in agricultural areas (such as crop substitution or variations caused

by different phenological stages in the agricultural cycle). The class Burned areas/shadow/ water show a decrease in Brightness and in Greenness components, since these types of targets in these two components remain dark. Deforestation can be detected by the decrease in Greenness component and an increase in component Brightness, as a result of a decrease of the participation of vegetation in the spectral response of the targets, with an increased participation of the soil. Through an overlay operation between the magnitude and direction in a GIS, a map of LULC changes between the years 1989 and 2010 was obtained (figure 7). The final map has five classes: biomass variation, burned areas/shadow/ water, deforestation, no change and regeneration.

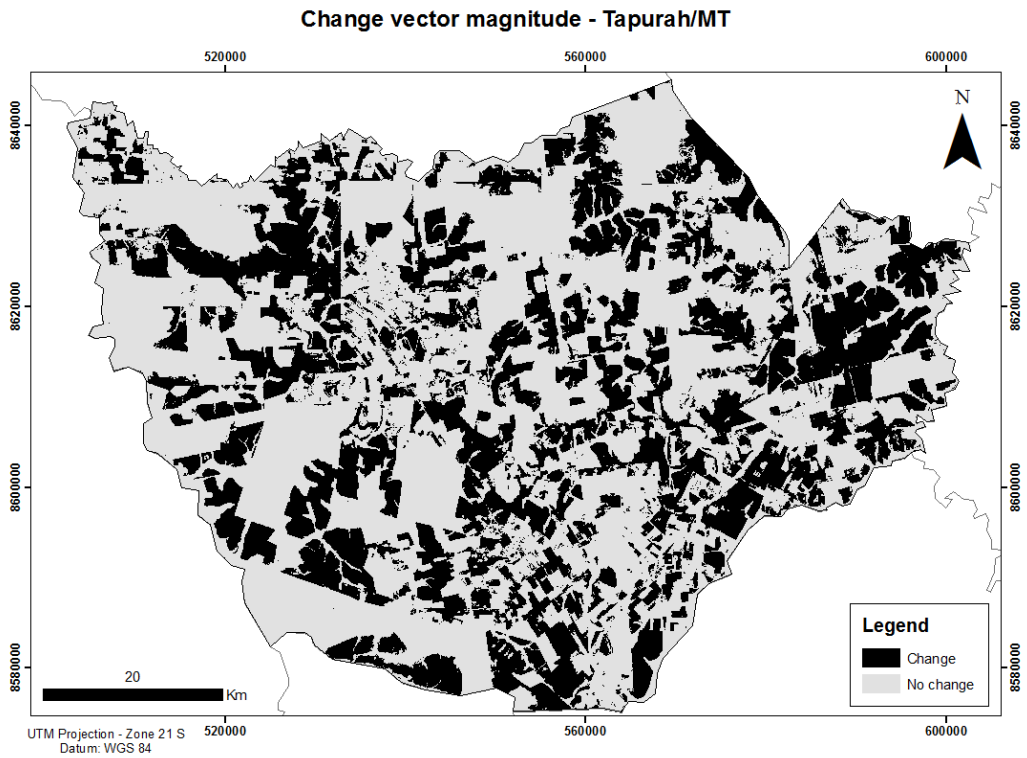


Fig. 5 – The change magnitude classified by the parallelepiped classification.

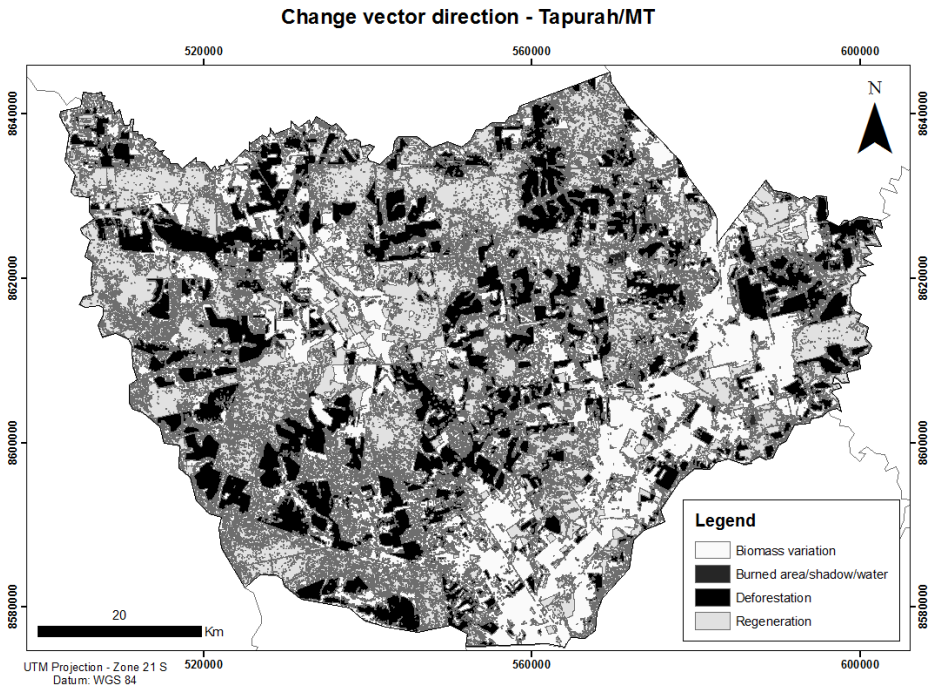


Fig. 6 – The vector direction classified after Density Slicing.

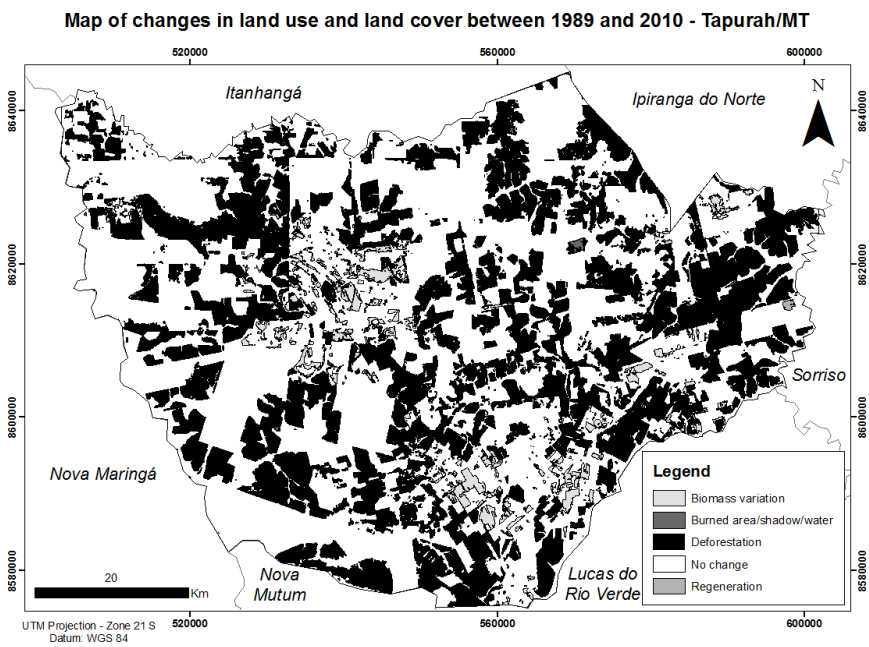


Fig. 7 – The final LULC change map obtained through CVA.

Table 6 shows the area percentage of each class. Approximately 33.9% of the city were cleared between 1989 and 2010 due to the advancement of agriculture, since the class deforestation, in the present work, is related to the reduction of native forest cover by the entry of agriculture.

LULC change	Percentage of the area (approximation)
Biomass variation	2,83%
Burned areas/shadow /water	0,14%
Deforestation	33,9%
No change	62,94%
Regeneration	0,2%

TABLE 6 – Percentage of the area of each LULC change class

## Evaluation

There was confusion between the map classes, specially among Deforestation and Biomass variation, as some agricultural areas in 1989 were with a high vegetative vigor (with a high value of Greenness), while in 2010, due to differences in the phenological cycle of crops, the vegetative vigor this time was low, which increased the spectral response of the soil, resulting in high values of Brightness. In this case, there was no change in the class, and false deforestation areas were detected. So there is this difficulty in agricultural areas, as if by chance the agricultural areas do not change, their spectral behavior varies over time depending on the developmental stage of the crop (JESUS; EPIPHANIO, 2010).

However, these incorrect classified areas were reclassified visually before generating the final map. After this reclassification, the map was evaluated based on 107 samples of reference. A hit of 85/107 samples was achieved, which allowed to obtain an overall accuracy of 0,7944. The map has Kappa index of 0,6464, which indicates a substantial classification according to Landis and Koch (1977).

The CVA allows the detection of deforestation and other changes in land use and land cover of Amazon effectively. This methodology allows deforestation detection quickly, which could help in the supervision of criminals deforestation.

## Conclusion

The hypothesis was confirmed. The CVA allowed the detection of deforestation caused by the expansion of agriculture in the Amazon environment (in this case, the municipality of Tapurah) effectively. The LULC change map generated by CVA between the analyzed period allowed the identification of five classes: Biomass variation, Burned area/shadow/water, Deforestation, No change and Regeneration.

The proposed method showed satisfactory results: the final map has a Kappa index of 0.6464, indicating a substantial classification. About 33.9% of the area of Tapurah was cleared due to the advancement of agriculture. Thus, Remote Sensing technologies are useful for monitoring deforestation.

#### References

- ALLEN, T. R.; KUPFER, J. A. Application of Spherical Statistics to Change Vector Analysis of Landsat Data: Southern Appalachian Spruce-Fir Forests. *Remote Sensing of Environment*, v.74, n.3, p.482-493, 2000.
- BAYARJARGAL, Y.; KARNIELI, A.; BAYASGALAN, M.; KHUDULMUR, S.; GANDUSH, C.; TUCKER, C. J. A comparative study of NOAA-AVHRR derived drought indices using change vector analysis. *Remote Sensing of Environment*, v.105, n.1 p.9-22, 2006.
- CHANDER, G.; MARKHAM, B. Revised Landsat-5 TM Radiometric calibration procedures and post-calibration dynamic ranges. *IEEE Transactions on Geoscience and Remote Sensing*, v.41, n.11, p.2674-2677, 2003.
- CHAVEZ, P. S. An improved dark-object subtraction technique for atmospheric scattering correction of multispectral data. *Remote Sensing of Environment*, v.24, n.3, p.459- 79, 1988.
- CONGALTON, R. G. A review of assessing the accuracy of classifications of remotely sensed data. *Remote Sensing of Environment*, v.37, n.1, p.35-46, 1991.
- CONGALTON, R. G.; GREEN, K. Assessing the accuracy of remotely sensed data: principles and practices. Boca Raton: Lewis Publishers, 1999. 137p.
- CRIST, E. P.; CICCONE, R. C. A physically-based transformation of Thematic Mapper data – the TM tasseled cap. *IEEE Transactions on Geoscience and Remote Sensing*, v.22, n.3, p.256-263, 1984.
- DEL CASTILLO, E. M. Uso e cobertura da terra numa região agrícola de Cerrado, via análise por vetor de mudança em imagens Landsat multitemporais. 2011. 143 p. (sid.inpe.br/mtc-m19/2011/05.27.01.43-TDI). Dissertação (Mestrado em Sensoriamento Remoto) - Instituto Nacional de Pesquisas Espaciais, São José dos Campos, 2011. Disponível em: <<http://urlib.net/8JMKD3MGP7W/39PC9ES>>. Acesso em: 13 jan. 2012.
- GLERIANI, J. M.; ANTUNES, M. A. H.; EPIPHANIO, J. C. N. Coeficientes da transformação espectral Tasseled Cap para uma cena com predomínio de latossolo roxo. In: SIMPÓSIO BRASILEIRO DE SENSORIAMENTO REMOTO (SBSR), 11., 2003, Belo Horizonte. Anais... São José dos Campos: INPE, 2003. Artigos, p. 101-107.
- GUERRA, A. J. T. Processos Erosivos nas Encostas. In: GUERRA, A. J. T.; CUNHA, S. B. (Org.). *Geomorfologia: Uma atualização de bases e conceitos*. 7. ed. Rio de Janeiro: Bertrand Brasil, 2007.
- HALL, F. G.; STREBEL, D. E.; NICKESON, J. E.; GOETZ, S.J. Radiometric rectification: toward a common radiometric response among multitemporal, multisensory images. *Remote Sensing of Environment*, v.35, n.1, p.11-27, 1991.
- IBGE. IBGE Cidades. Disponível em: <[www.ibge.gov.br/cidadesat/](http://www.ibge.gov.br/cidadesat/)>. Acesso em: 15 jan. 2012.
- JEPSON, W. A disappearing biome? Reconsidering land cover change in the Brazilian savanna. *The Geographical Journal*, v.17, p.99–111, 2005.
- JESUS, S. C. Análise por vetor de mudanças para a avaliação multitemporal e multissensores da cobertura das terras do cerrado. 2009. 97 p. (INPE-16597-TDI/1583). Dissertação (Mestrado em Sensoriamento Remoto) - Instituto Nacional de Pesquisas Espaciais, São José dos Campos, 2009. Disponível em: <<http://urlib.net/sid.inpe.br/mtc-m18@80/2009/10.21.10.27>>. Acesso em: 13 jan. 2012.
- JESUS, S. C.; EPIPHANIO, J. C. N. Sensoriamento remoto multissensores para a avaliação temporal da expansão agrícola municipal/Remote sensing for multitemporal analysis of agricultural expansion. *Bragantia*, v. 69, n. 4, p. 01-02, 2009.
- JIANYA, G.; HAIGANG, S.; GOURUI, M.; QUIMING, Z. A review of multi-temporal remote sensing data change detection algorithms. *International Archives of the Photogrammetry, Remote Sensing and Spatial Information Sciences*.v.37. n.B7, 2008.

- JOHNSON, R. D.; KASISCHKE, E. S. Change vector analysis: a technique for the multispectral monitoring of land cover and condition. *International Journal of Remote Sensing*, v.19, n.3, p.411-426, 1998.
- KAUTH, R. J.; THOMAS, G. S. The tasseled cap – a graphic description of the spectral temporal development of agricultural crops as seen in Landsat. In: SYMPOSIUM ON MACHINE PROCESSING OF REMOTELY SENSED DATA, 1976, West Lafayette, Indiana. Proceedings... West Lafayette: [s.n.], 1976. p.41-51.
- LANDIS, J. R.; KOCH, G. G. The measurement of observer agreement for categorical data. *Biometrics*, v.33, p.159–174, 1977.
- LU, D.; MAUSEL, P.; BRONDÍZIO, E.; MORAN, E. Change detection techniques. *International Journal of Remote Sensing*, v.25, n.2, p.2365- 2407, 2004.
- MALILA, W. A. Change Vector Analysis: an approach for detecting forest changes with Landsat. In: Machine Processing of Remotely Sensed Data Symposium, LARS, Purdue University, West Lafayette, 1980. Proceedings... Indiana, p. 2b25 – 2b37, 1980.
- MICHALEK, J. L.; LUCZKOVICH, J. J.; STOFFLE, R. W. Multispectral Change Vector Analysis for monitoring coastal marine environments. *Photogrammetric Engineering and Remote Sensing*, v. 59, n. 3, p. 381-384, 1993.
- MESQUITA JÚNIOR, H. N.; SILVA, M. C.; WATANABE, N. Y.; ESTEVES, R. L. Aplicações de sensoriamento remoto para o monitoramento do desmatamento da Amazônia. In: SIMPÓSIO BRASILEIRO DE SENSORIAMENTO REMOTO, 13. (SBSR), 2007, Florianópolis. Anais... São José dos Campos: INPE, 2007. p. 6835-6842. CD-ROM, On-line. ISBN 978-85-17-00031-7. Disponível em: <<http://urlib.net/dpi.inpe.br/sbsr@80/2006/11.15.23.56.56>>. Acesso em: 13 jan. 2012.
- PRAKASH, A.; GUPTA R. P. Land-use mapping and change detection in a coal mining area - a case study of the Jharia coalfield, India. *International Journal of Remote Sensing*, v.19, p.391-410, 1998.
- PONZONI, F. J.; SHIMABUKURO, Y. E. Sensoriamento remoto no estudo da vegetação. p.144. São José dos Campos - SP: Editora Parêntese, 2009.
- RADAMBRASIL. Folha SD.21 Cuiabá: vegetação. Rio de Janeiro, 1982. 544p. (Levantamento de Recursos Naturais, 26).
- SINGH, A. Digital change detection techniques using remotely-sensed data. *International Journal of Remote Sensing*, v.10, p.989–1003, 1989.
- SOHL, T. Change analysis in the United Arab Emirates: an investigation of techniques. *Photogrammetric Engineering and Remote Sensing*, v.65, n.4, p.475-484, 1999.
- XIAN, G.; HOMER, C.; FRY, J. Updating the 2001 National Land Cover Database land cover classification to 2006 by using Landsat imagery change detection methods. *Remote Sensing of Environment*, v. 113, n.3, p. 1133-1147, 2009.